Magnetic Resonance Propulsion, Control and Tracking at 24 Hz of an Untethered Device in the Carotid Artery of a Living Animal: An Important Step in the Development of Medical Micro- and Nanorobots

Sylvain Martel, *Senior Member, IEEE*

NanoRobotics Laboratory, Department of Computer Engineering and Institute of Biomedical Engineering, École Polytechnique de Montréal (EPM), Campus of the Université de Montréal, Montréal, Canada

E-mail: sylvain.martel@polymtl.ca URL: www.nano.polymtl.ca

***Abstract*—Our recent demonstration of a ferromagnetic bead being navigated automatically inside the carotid artery of a living animal at an average speed of 10 cm/s using a clinical MRI system may be considered as a significant step in the field of medical micro- and nanorobotics. This is particularly true when we consider that an appropriate tracking method was embedded in the closed-loop control process allowing the blood vessels to be considered as navigational routes, providing maximum access for conducting operations inside the human body. But more importantly, this demonstration not only validates preliminary theoretical models but provides us with initial insights about the strategies and approaches that are likely to be used to navigate under computer control, micro- and nanodevices including nanorobots from the largest to the smallest diameter blood vessels that could be used to reach targets inside the human body. Here, based on these initial experimental data obtained *in vivo*, such strategies and methods are briefly described with some initial design concepts of medical interventional micro- and nanorobots.**

***Index Terms*—Micro- and nanorobots, magnetic resonance imaging, magnetic gradients, blood vessels, targeted therapies**

I. Introduction

The feasibility for *in vivo* navigation of untethered devices including robots was demonstrated in [1] with the automatic closed-loop control and tracking of a 1.5 mm diameter ferromagnetic bead in the carotid artery of a living swine. During the experiments, the three orthogonal slice selection and signal encoding gradient coils of a standard clinical Magnetic Resonance Imaging (MRI) platform were used to induce a force on the ferromagnetic material, a technique described in more details in [2]. But more importantly, although there are several research publications describing the manipulation, orientation, and displacement of untethered objects using magnetic fields, none has suggested an approach that includes an imaging modality allowing closed-loop control inside the vascular network. More recently, the need for closed-loop control in medical microrobotics has also been recognized in [3] where magnetically controlled untethered robots have been designed for future intraocular procedures using visual feedback through direct line of sight through the pupil. But the use of a clinical MRI system for both propulsion and imaging modality for untethered medical micro- and nanorobots offers potentials for many types of medical interventions while offering many advantages compared to other imaging modalities for tracking them in the human body where direct line of sight is not possible [4]. They include but are not limited to three-dimensional imaging, enhanced tissue contrast, lack of radiation, and widespread availability in clinical environments.

II. Medical Microrobots

A. Level of Autonomy

Although the literature defines robots in many ways, they can be defined as moving devices that can make decisions by processing incoming information. As such, an untethered robot must not just have the capability to move or travel in the blood vessels, but must take advantage of the capability to capture and process information needed to accomplish its mission, as well as be designed to operate within specific constraints (including technological and physiological constraints). Our studies so far indicate that several control actions will be required per second taking into account many parameters. For instance, in [1], the navigation of a 1.5 mm bead in a 5 mm inner diameter carotid artery of a living swine was done at 24 Hz. This suggests that a computer-controlled approach without human interventions during the real-time control or navigation process is much more adequate considering parameters such as precision and safety, to name but only two, than a tele-operated approach where a surgeon for instance could steer these robots using apparatus such as joysticks. As a simple example, if a ferromagnetic core is navigated in a too large blood vessel, the induced force on the ferromagnetic core may not be sufficient to counteract the larger blood flow typically

encountered in larger vessels. As a result, the surgeon would lose control and the device may end up blocking blood flow to critical parts of the brain for instance. On the contrary, the same results may occur if the ferromagnetic core is navigated in a too small diameter vessel taking also into consideration retarding effect of the vessels walls that may become predominant and reduces the magnetophoretic velocity. This suggests that the future surgeon may be involved in the planning phase using specialized software prior to the interventions but once the devices or robots are introduced in the vascular network, the whole process would become fully autonomous with several decisions based on specific rules being made per second.

B. Dimensions

One fundamental rule is to navigate a robot within acceptable vessels diameters relative to the diameter of the robot itself. For a given blood vessel, the maximum magnetophoretic velocity occurs for a *d*/D ratio (the diameter *d* of the device being navigated vs. the diameter *D* of the vessel) between approximately 0.4 and 0.5. Considering the range in diameters of the various blood vessels (~25 mm dia. for the aorta and down to ~5 μm dia. for the smallest capillaries), indicates that such robots must not only have the capability to agglomerate or dissociate from previous agglomerations to increase the induced propulsion force when navigating in larger diameter vessels, but each one of these microrobots could require overall size diameter as small as ~2 μm. This may suggest agglomerations in the form of a ferrofluid.

B. Embedded Intelligence

In the context of robotics, although actual technological limitations prevent us to embed enough "intelligence" within such small devices or robots (considering other aspects such as power source), the fact that "intelligence" is implemented outside while maintaining the capability of influencing their behaviors, still may be within the definition of microrobots. Nonetheless, even if an extremely high level of "intelligence" could be embedded in these microrobots, they would still need an external system to guide them in this maze that represents the human vascular network made of approximately 80,000 km of blood vessels, especially during direct targeting applications. In fact, medical untethered microrobots have the potential to play a significant role in these applications such as enabling a variety of localized treatment and diagnostic modalities while at the same time reducing undesired side effects.

III. MEDICAL NANOROBOTS

Going further than microrobots, it is relatively well recognized in the scientific community that a nanorobot is not necessarily a robot with overall dimensions in the nanometer-scale but one that depends on parts of nanoscale dimensions or one that relies on nanotechnology to embed functionalities that otherwise could not be implemented. This is somewhat similar to nanotechnology that would rely on nanoscale components to build larger devices or components having different properties.

In fact, nanotechnology including nanomedicine can influence the design and development of medical nanorobots in many ways. For most applications, the main body of micrometer-sized robots would consist of magnetic nanoparticles embedded in a material such as a polymer. These nanoparticles enable multiple, distinct therapeutic functions and are used for propulsion and steering of the nanorobots, RF hyperthermia and MRI contrast enhancement, allowing the nanorobots to be tracked and hence, enabling closed-loop control.

A. Motion

The motion of the untethered nanorobots is governed by several factors including the magnetic force, viscous drag, robot-blood cell interactions, thermal kinetics or Brownian motion, nanorobot-fluid interactions or perturbations to the flow field, inter-nanorobot effects such as magnetic dipole interactions, and much less dominant effects (compared to larger untethered robots) such as inertia, buoyancy, and gravity. Although the latter factors constrained the performance of the *in vivo* experiment described in [1] using a 1.5 mm diameter bead navigated in an artery, they are not a real concern when smallest objects or robots are being navigated in the microvasculature. On the other hand, beside other factors listed earlier and influencing motion at such a scale, since magnetic force scales down at a cubic rate while drag force decreases linearly at low Reynolds numbers, the addition of propulsion dedicated gradient coils in the MRI bore must be considered. But due to limits in gradient amplitudes that can be generated, steering instead of propelling nanorobots in the microvascular network seems to be a more logical approach in this context. At such a scale, blood is no longer homogeneous and in the smallest capillaries, the overall dimension of a single nanorobot is smaller than a red cell.

Although 10 round-trips were done in the carotid artery [1], unidirectional motion of the nanorobots between red cells following blood flow with induced steering force at vessel bifurcations must be considered. Enhanced steering capability can also be achieved by increasing the volume of ferromagnetic or superparamagnetic material through tightly coupled agglomeration of nanorobots (taking advantages of the forces involved at such a scale) and by a reduction of the blood flow using temporary embolization.

B. Tracking

When not at the nanometer-scale, ferromagnetic material creates significant MR image artifacts that prevents adequate tracking and hence, proper navigational control of the robot [5]. As such, a new MR tracking technique [6]

with sufficient real-time performance allowing precise tracking and control by eliminating MR image artifacts was developed for applications in larger blood vessels and was validated *in vivo* in [1]. The tracking technique although successful has two major drawbacks. First, the technique demands a fair amount of computation which may have in some cases, an impact on the real-time performance. Second, although it can track in real-time the position of larger ferromagnetic entity inside the body with relatively high precision, the position must be superimposed on an image previously taken using MRI or another medical imaging modality, preventing the use of reference points close and inside the body for registration purpose. But nanoparticles in smallest medical untethered robots behave like MRI contrast agent due to their single domain magnetic property that already proved to be visible and traceable with MRI without causing image artefacts as it is the case for larger magnetic entities. Without MR image artefacts surrounding the nanorobots, registration techniques inside the body can be considered. The concentration of nanorobots must be sufficient not only to provide additional steering force and to deliver adequate doses of therapeutic agents but also to increase the signal from the nanoparticles to a level sufficient to be detected by MRI.

C. Multi-functionality

RF hyperthermia with the use of nanoparticles offers the possibility of increasing temperature at selected sites to improve therapeutic efficacy and can be used as a computer-triggered drug release mechanism for nanorobots beside the use of time-specific biodegradable polymer or polymer reacting to specific environmental changes (e.g. pH level in tumoral lesions). Nanomedicine and biochemistry including progress in chemo-, radio- and gene therapy will further influence the design of such medical nanorobots. A simple fundamental example of such nanorobots is depicted in Fig. 1. Fundamentally, it consists of a nonmagnetic core material with embedded magnetic nanoparticles. The nonmagnetic core can be made of various materials including biodegradable polymers such as PLA or PLGA (see Fig. 1), or other material such as polyarcylamide (PAA). Therapeutic agents can also be added and biotargeting agents can be coated onto the surface to control plasma residence time.

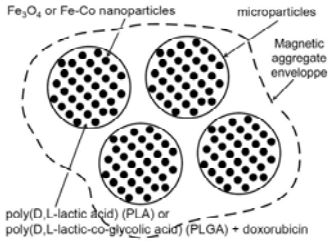

Fig. 1. One among several possible examples of steered ferromagnetic nanorobots here shown without therapeutic or biotargeting/biosensing agents.

One example is to include multifunctional micelles to provide effective cancer targeting with ultra-sensitive detection by MRI as described in [7].

The magnetic material embedded inside the magnetic particles has a direct effect on the magnetic force. Iron Oxide (Fe_3O_4) has been used extensively in the literature. Nevertheless, Iron Cobalt (FeCo) magnetic particles are 4 times more sensitive to the magnetic gradient and can be formulated as nanoparticles. Although various sizes can be synthesized, a lower diameter of 10 nm [8] seems to be to lowest limit to achieve equal concentrations of Fe and Co required for achieving the most effective level of induced force on each particle. The main drawback associated with their usage is the toxicity of cobalt ions that might reduce the dosage translating to a maximum limit to the number of microrobots that could be administered to a patient unless a protective layer is considered in the design. The density of nanoparticles within each microdevice can also be adjusted to provide different velocities among devices in the same agglomeration.

IV. General Targeting Strategy

A. Experimental Data on Targeting in Larger Blood Vessels

It was shown by our group that targeting in larger blood vessels is possible [1] as shown in Fig. 2 and Fig. 3.

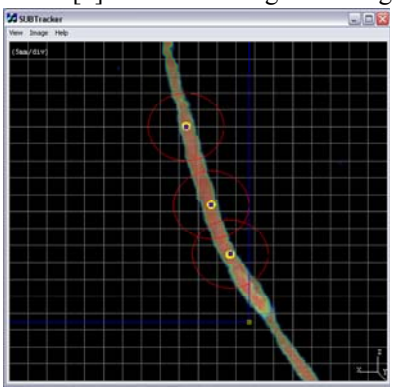

Fig.2. Carotid artery of a living swine taken by MRI and processed though special software modules showing way-points where a 1.5 mm ferromagnetic bead was navigated by computer and tracked at 24 Hz while doing 10 pre-planned round-trips at an average speed of 10 cm/s.

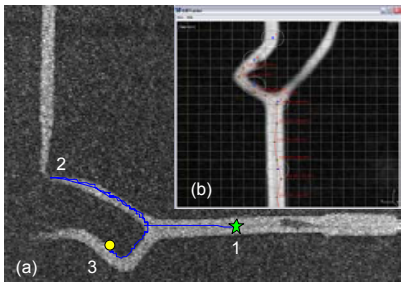

Fig. 3. (a) MR image of a vascular phantom taken with a contrast agent (gadolinium) whose dimensions is 500 × 500 pixels (1 pixel = 0.4883 mm × 0.4883 mm) with the trajectory of the microrobot trajectory in the artificial blood vessel being superposed at 30 Hz on the image. (b) Example of the blood vessels taken from the clinical MRI system and filtered as it appears on the user interface with waypoints plotted along the planned trajectory.

Fig. 3 shows that more complex trajectories are also possible. Although *in vivo* tests were performed on a 25 kg living swine, the vascular phantom mimicking a real human vasculature with blood vessels inner diameters varying between approximately 5 to 8 mm as depicted in Fig. 3 suggests that the same techniques can be applied to human. Fig. 3a shows the horizontal trajectory of the same ferromagnetic robot (or bead) inside a vascular phantom which is guided and propelled by the imaging gradients coils (40 mT/m) of a Siemens Avanto 1.5 T clinical MRI system using a real-time feedback controller relying on an echo gradient tracking sequence. The navigated robot was assigned a trajectory through a series of waypoints set on a computer display as depicted by an example in Fig. 3b which departs from its initial position in the main phantom's segment (position 1 in Fig. 3a) to a waypoint in the upper segment (position 2 in Fig. 3a) and then to the final waypoint in the lower segment (position 3 in Fig. 3a).

B. Targeting Strategy in the Microvasculature

A simplified schematic of the various types of blood vessels used to reach the tumoral lesion is depicted in Fig. 4. The diagram also suggests that better efficacy will be achieved through various types of nanorobots. For instance, when agglomerated or injected in the vicinity of the arterioles, targeting nanorobots must travel faster than embolization nanorobots when subjected to the same magnetic gradients. This can be accomplished by increasing drag force (varying the overall size, shape, etc.) and adjusting the amount of ferromagnetic nanoparticles embedded on each type of nanorobots. The difference in speed will allow targeting nanorobots to enter capillaries prior to temporary embolization that will facilitate steering through a decrease of the blood flow. Embolization or chemo-embolization nanorobots would typically be made of biodegradable polymer set to degrade at a specific time. Small diameter vessels are presently not visible on any medical imaging systems making the path planning more challenging. Hence, although such nanorobots can be imaged in an MRI system, effective path planning to reach the target is necessary to avoid a potential contamination through a too large quantity of robots being injected. As such, "scout" nanorobots similar to the ones described here but with minimum toxic compounds could be envisioned.

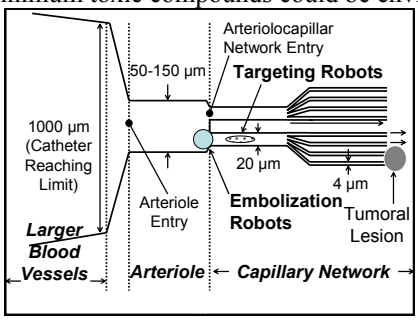

Fig. 4. Simplified schematic of the various types of blood vessels that need to be accessed prior to reach to tumoral lesion.

V. CONCLUSION

Unlike previous studies of medical micro- nanorobots in human blood vessels, here we show that the real challenge goes beyond actuation and control and must address the integration of many inter-disciplinary components within tight real-time, technological and physiological constraints. Various types of nanorobots with different dimensions are also required to effectively navigate in the various diameters vessels of the human blood network. We also demonstrated through preliminary experimental results that it is possible to propel or steer agglomerations of ferromagnetic nanorobots in blood vessels using magnetic gradients from a clinical MRI system providing imaging modality inside the human body to allow closed-loop navigational control.

ACKNOWLEDGMENT

The author acknowledges financial support from the Natural Sciences and Engineering Research Council of Canada (NSERC), the Canada Research Chair (CRC) in Micro/Nanosystem Development, Fabrication and Validation, the Canada Foundation for Innovation (CFI), and the Government of Québec.

REFERENCES

[1] S. Martel, *et al.*, "Automatic navigation of an untethered device in the artery of a living animal using a conventional clinical magnetic resonance imaging system," *Applied Physics Letters*, vol. 90, 114105, March 12, 2007

[2] J.-B. Mathieu, G. Beaudoin, and S. Martel, "Method of propulsion of a ferromagnetic core in the cardiovascular system through magnetic gradients generated by an MRI system," *IEEE Transactions on Biomedical Engineering*, vol. 53, no. 2, pp. 292-299, Feb. 2006

[3] K. B. Yesin, P. Exner, K. Vollmers, and B. J. Nelson, "Design and control of in-vivo magnetic microrobots," *In Proc. of the 9th Int. Conf. for Medical Imaging Computing, Computer-Assisted Intervention and Medical Robotics (MICCAI),* pp. 819-826, 2005

[4] S. Martel *et al.*, "Adapting MRI systems to propel and guide microdevices in the human blood circulatory system," *In Proc. of the of the 26th Annual Int. Conf. of the IEEE Eng. in Medicine and Biology Society (EMBS)*, San Francisco, USA, pp. 1044-1047, Sept. 1-5, 2004

[5] O. Felfoul, J. B. Mathieu, S. Martel, and G. Beaudoin, " Micro-device's susceptibility difference based MRI positioning system, a preliminary investigation," *In Proc. of the 26th Annual Int. Conf. of the IEEE Eng. in Medicine and Biology Society*, San Francisco, pp. 1140-1143, Sept. 1- 5, 2004

[6] E. Aboussouan and S. Martel, "High precision absolute positioning of medical instruments in MRI systems," *In Proc. of the 28th Annual Int. Conf. of the IEEE Engineering in Medicine and Biology Society*, New York, USA, Aug. 30-Sept. 3, 2006

[7] N. Nasongkla, *et al.*, "Multifunctional polymeric micelles as cancer-targeted, MRI-ultrasensitive drug delivery systems," *Nano* Letters, vol. 6, no. 11, pp. 2427-2430, 2006

[8] A. Hütten, *et al.*, "Ferromagnetic FeCo nanoparticles for biotechnology," *Journal of Magnetism and Magnetic Materials*, vol. 293, pp. 93-101, 2005